

Growth of ZnGa₂O₄ Phosphor by Radio Frequency Magnetron Sputtering

I. J. Hsieh

Department of Electrical Engineering, Chung-Hua Polytechnic Institute, Hsinchu, Taiwan

M. S. Feng, K. T. Kuo, and P. Lin

Institute of Materials Science and Engineering, National Chiao Tung University, Hsinchu, Taiwan

ABSTRACT

ZnGa₂O₄ films have been prepared by radio frequency (RF) magnetron sputtering at various total pressure, RF power, and substrate temperatures. Microstructure and crystallographic orientation were characterized by x-ray diffraction. Surface morphologies were observed by scanning electron microscope. In addition, cathodoluminescence (CL) measurement was employed to observe the emission spectra of ZnGa₂O₄ films. The influences of various deposition parameters on the properties of grown films were studied. The optimum substrate deposition temperature for luminous characteristics was about 500°C in this investigation. A blue cathodoluminescent emission peaked at 470 nm was observed. Good luminescent properties were observed in the films which exhibit the standard ZnGa₂O₄ x-ray diffraction pattern.

Field emission display (FED) is a new kind of vacuum flat cathode ray tube. Due to the attractive advantage of FED, it is a good candidate for replacing conventional cathode ray tube (CRT) in flat panel display. In FED, light emission is based on low voltage cathodoluminescence.^{1,2} Usually, phosphors show a decrease in cathodoluminescent efficiency as the accelerating voltage is reduced, especially below 1 kV. Low-voltage (of the order of 50 V) CL phosphors have also attracted substantial interests for the reduction in accelerating voltage in cathode tubes.³⁻⁵ The ZnGa₂O₄ phosphor has been investigated for its good cathodoluminescence characteristics at low voltage. A luminous efficiency of 0.7 lm/W has been obtained when this phosphor is operated at 30 V dc. The results of high temperature operating lifetime test have been proven to show the excellent stability of this phosphor. In addition, ZnGa₂O₄ shows emission from green to red when it is doped with Cr and Mn, and also shows blue emission even without being doped with impurity. The conventional phosphors have been prepared by powder metallurgy. In the recent development, the thin films of ZnGa₂O₄ phosphor were of interest for the applications of FED. The properties of phosphors are strongly dependent on the particle size and crystal structure,^{6,7} and the growth conditions may be adjusted to achieve better luminescent characteristics.

In this work, the technique of sputtering was employed to deposit ZnGa₂O₄ phosphor films. The sputtering condition were adjusted for investigating the relationship among deposition condition, deposition rate, and luminescent characteristics.

Experimental

ZnGa₂O₄ thin films were prepared by reactive sputtering in a conventional radio frequency (RF) magnetron sputtering apparatus. A water-cooled powder target (3 in. diam, 99.999% purity) was used as a target. ZnO and Ga₂O₃ powder (99.999% purity) were mixed in 1:1 proportion. The mixed powder was then ball-milled in acetone for 24 h and dried by IR lamp. Then the pulverized powder was packed and pressed into a stainless dish. The ball-milled powder was mixed with DI water and baked at 150°C for 2 h before filling the dish. n-Type, (100) Si wafers, and Corning 7059 glass (5 × 5 cm) were used as substrates. The substrates were thoroughly cleaned by the standard RCA procedures.

Table I. Sputtering parameters.

RF power	50 to 250 W
Total pressure	1 to 20 mTorr
Oxygen ratio	0 to 40%
Substrate temperature	200 to 600°C
Flow rate	20 sccm

Oxygen and argon were used as reactant and working gases. The gases with desired pressure and ratios were allowed to flow for 10 min to purge the chamber. Thin film deposition was started by removing the shutter from substrate after the target had been cleaned by argon plasma sputtering for 20 min. The deposition parameters are listed in Table I. Various parameters, such as working pressure, substrate temperature, RF power, and gas ratios, have been varied to study the growth of ZnGa₂O₄ films. To further investigate the annealing effects on phosphor films, some of the films were annealed in an air furnace at various temperatures and different times.

The thickness of deposited films was measured by Sloan Dektak 3030 alpha-step surface profile with low scanning speed and 10 mg load at various places on the films. A Hitachi S2500 scanning electron microscope equipped with energy dispersive spectrometer (Kevex-EDS) was used for the observation of surface morphology and the estimation of gallium/zinc composition ratios. The phase identification of grown films was carried out by an x-ray diffractometer (Siemens D5000) with Cu-Kα first radiation.

An ABT-150S-type scanning electron microscope equipped with a cathodoluminescence system was used for the emission spectra measurement in different accelerating voltage (5 kV to 500 V) at room temperature to observe the emission behavior of ZnGa₂O₄ phosphors. The low voltage cathodoluminescence (LVCL) measurement conditions were accelerating voltage: 500 V, emission current: 20 μA, magnitude: 300 times. The wavelength range of emission spectra was 300 to 700 nm.

Results and Discussion

The deposition rate *vs.* power was shown in Fig. 1. The deposition rates were found to be increased with increasing

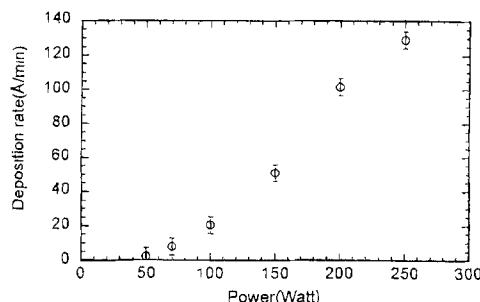


Fig. 1. Deposition rates of the ZnGa₂O₄ film grown at different RF powers.

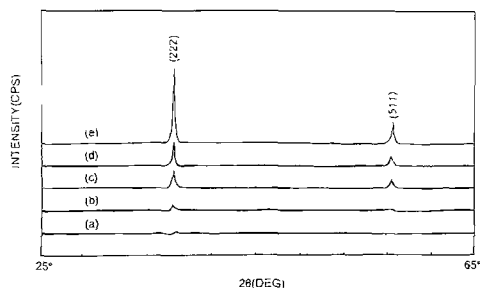


Fig. 2. XRD patterns of the film deposited at different RF powers (a) 30, (b) 50, (c) 70, (d) 100, and (e) 150 W, with fixed deposition time constant and with fixed total pressure, and no substrate heating.

RF generating power. Increasing the RF power dissipated in the plasma increases the sheath potential and increases the concentration of reactive argon ions. Then more sputtered atoms due to argon plasma bombardment are introduced to the surface. Deposition rates therefore normally increase almost linearly with increasing power. So, the higher power value led to higher deposition rate.⁸ The corresponding x-ray diffraction patterns by powder method for the ZnGa_2O_4 films deposited under various RF powers with fixed deposition time constant, fixed total pressure, and no substrate heating are shown in Fig. 2, demonstrating the crystal orientation distribution of ZnGa_2O_4 films. A strong (222) preferred orientation is observed. Meanwhile, the peak intensity of (222) preferred orientation is higher for the film deposited with higher RF power, indicating the consistency between preferred orientation and film thickness.

Figure 3 shows the deposition rate as a function of total gas pressure. The lower deposition rate was found as the total pressure was increased. In particular, the deposition rate was significantly reduced at 20 mTorr. Eventually, the gas pressure is a key factor for determining the deposition rate in the vapor-phase deposition. Since surface scattering phenomenon becomes obvious as the total pressure increases by increasing the total pressure, the collision probability among the gas atoms would be raised before they arrive at the substrate. Thus, more scattering events would be expected for higher pressure. As a result of scattering, the momentum and mobility of adhere atoms on the substrate are reduced.⁹ If the operating pressure is too high, the mean free path (MFP) of the sputtered atom will be short, and the probability of it being backscattered to the target will be increased. So the formation of phosphor film would be more difficult.

From the kinetic theory of gases, MFP (λ) is calculated as¹⁰

$$\lambda = \frac{kt}{p\pi\sigma^2\sqrt{2}}$$

where k is Boltzmann's gas constant, T is the temperature in degrees Kelvin, p is the pressure, and σ is the molecular diameter. At room temperature, we can estimate approxi-

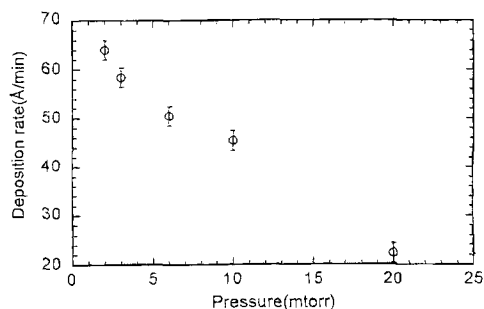


Fig. 3. Deposition rate as a function of pressure.

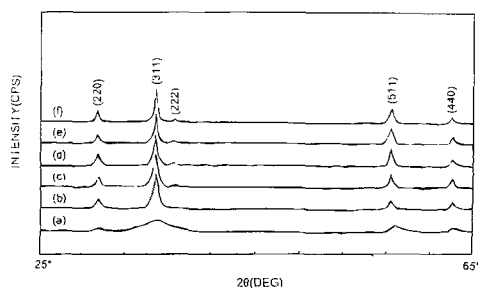


Fig. 4. XRD patterns of different oxygen ratios: (a) 0, (b) 2.5, (c) 5, (d) 10, (e) 15, and (f) 20%.

mately the MFP as a function of pressure as the following relation

$$\lambda \approx \frac{5.2 \times 10^{-3} \text{ cm}}{P(\text{Torr})}$$

The MFP ($\lambda \approx 0.26$ cm) at 20 mTorr is much smaller than the distance between target and substrate ($d = 6$ cm). Hence, the deposition rate was significantly reduced at 20 mTorr.

Figure 4 shows a series of XRD patterns of ZnGa_2O_4 films grown under various Ar/O_2 flow rate ratio with fixed gas pressure (3 mTorr), RF power (150 W), substrate temperature (500°C), and deposition time (2 h). It seems that the oxygen environment is necessary for achieving the films with good crystallinity.

The temperature effect on the structure of deposited films measured by XRD is shown in Fig. 5. As the substrate temperature rises, the intensity of main peak (311) increases. A transition temperature at 300°C is observed. The (222) peak almost disappears when temperature is higher than 500°C. For the x-ray diffraction patterns of ZnGa_2O_4 (311) is the main peak of standard powder diffraction pattern and (222) is the preferred orientation of the film deposited on Si (100). It is probable that the high substrate temperature destroys the preferred orientation and leads to powder distribution of deposited films. In addition, it was also found recently that better cathodoluminescent characteristics were achieved from the films with standard powder diffraction pattern of ZnGa_2O_4 .

In Fig. 6, Ga/Zn ratio was found to be dependent on the substrate temperature. The Ga/Zn atomic ratio is larger when the substrate temperature increases. We know that the vapor pressure of Zn is higher than that of Ga.¹¹ As the growth temperature is raised, the Zn atoms would have more opportunities to diffuse out. It would make deposited films convert to excess gallium content condition. It was also found that the structure with excess gallium had excellent cathodoluminescent characteristics.

Figure 7 shows the room temperature LVCL (500 V) spectra of phosphor films grown at different temperatures. It was found that the sample grown at higher temperature has higher luminescent intensity. In addition, the cathodoluminescent spectra of the samples grown at higher temperature are composed of three main emission peaks, ${}^2\text{E} \rightarrow {}^4\text{A}_2$,

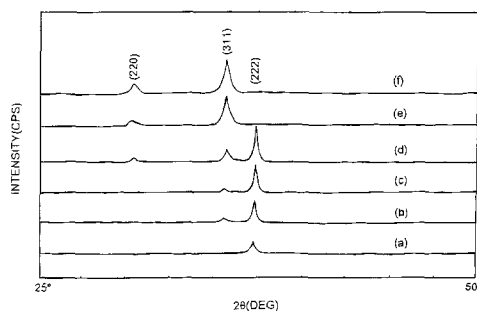


Fig. 5. XRD patterns for different substrate temperatures (a) no heating, (b) 200, (c) 300, (d) 450, (e) 500, and (f) 600°C, at 150 W, 4 mTorr and 10% O_2 .

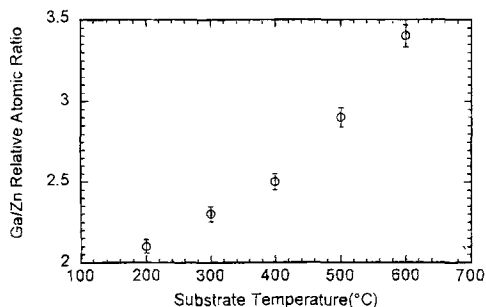


Fig. 6. Ga/Zn relative ratio vs. substrate temperature for the deposited phosphor film.

${}^4T_2 \rightarrow {}^4A_2$, and ${}^4T_1 \rightarrow {}^4A_2$. These emission spectra can be correlated with the results in Fig. 5 and 6. From Fig. 5, different growth temperatures may result in two kinds of x-ray diffraction, indicating the structures of grown films are different if they are deposited above and below 500°C. High growth temperature leads to large Ga/Zn ratio, as shown in Fig. 6. So we propose that the excess Ga content acts as the activators. The effect of Ga³⁺ ions is just like Cr³⁺ ion in spinel structure.¹² The wave functions of the S, P, D . . . terms are similar to those for s, p, d . . . orbitals, because the terms differ slightly from those of the corresponding orbitals, and thus they may transform differently in a particular point group. For the octahedral structure, for example, whereas p orbitals transform as T_{1u} , the P term derived from the d configuration transforms as T_{1g} . The way in which the various terms transform is given by the methods previously outlined for orbitals.¹³ The geometrical arrangements of the five 3d orbitals become significant, since the interactions with the orbitals of the six oxygen ligands will result in shifts in the energy levels of the individual orbitals. The energy levels split, so that the five 3d levels no longer have the same energy. The most commonly observed octahedral or tetrahedral environments lead to different

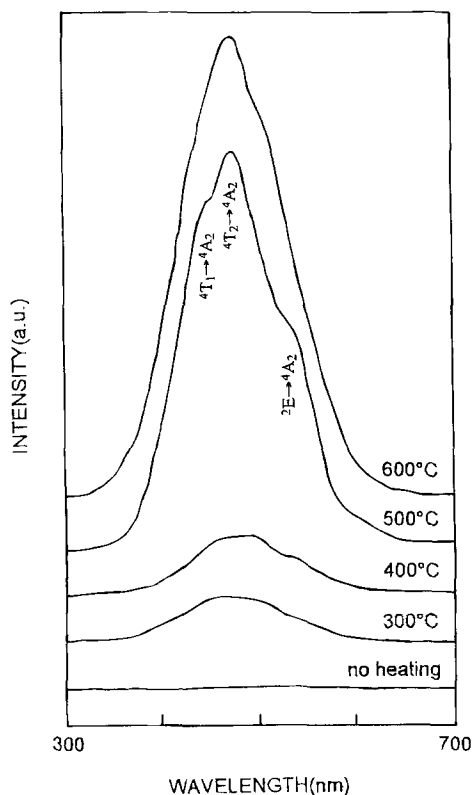


Fig. 7. Room temperature LVCL (500 V) spectra of ZnGa₂O₄ films (150 W, 4 mTorr, Ar/O₂ = 18/2) grown at different substrate temperatures.

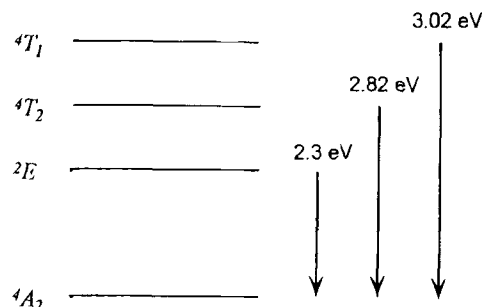


Fig. 8. Proposed energy level diagram of ZnGa₂O₄ for cathodoluminescent spectra.

arrangements.¹⁴ The effect of the strength of the ligand field on the resulting energy levels, labeled by their spectroscopic terms 4A_2 , 4T_1 , 4T_2 , and 2E , is shown in the term diagram of Fig. 8. With respect to the ground level 4A_2 as the zero of the field, the energy of the 2E level changes very little with the strength of the field, but the 4T_1 and 4T_2 levels change significantly. It means the change between octahedral and tetrahedral structures. The main transition in this kind of structure is the ${}^4T_2 \rightarrow {}^2A_2$ emission.^{15,16} But in Fig. 7, we can find two weak peaks that might be represented 4T_1 and 2E . So inorganic phosphors are made by doping certain host materials with activators such as Ag⁺, Cu⁺, Mn²⁺, or Cr³⁺ ions. It had been reported that spinel structure doped with Mn²⁺ and Cr³⁺ ions emitted green and red light.^{17,18}

The emission spectra of the films before and after annealing have been compared. Figure 9 shows the 500 V accelerating voltage CL spectra of phosphor films annealed at different temperatures. Much better low voltage CL characteristics were achieved after the annealing treatment. The main peak of the x-ray diffraction patterns for as-grown and annealed samples shown in Fig. 10 changed from (222) peak to (311) peak. Figure 11 is LVCL spectra of phosphor films (150 W, 4 mTorr, Ar/O₂ = 18/2, and 600°C) annealed at different temperatures for 3 h. The main transition peak shift from 470 to 360 nm. As discussed above, orbitals have specific shapes and geometrical configurations in space. The fact that the five 3d orbitals pointed in different directions had no significance to an isolated

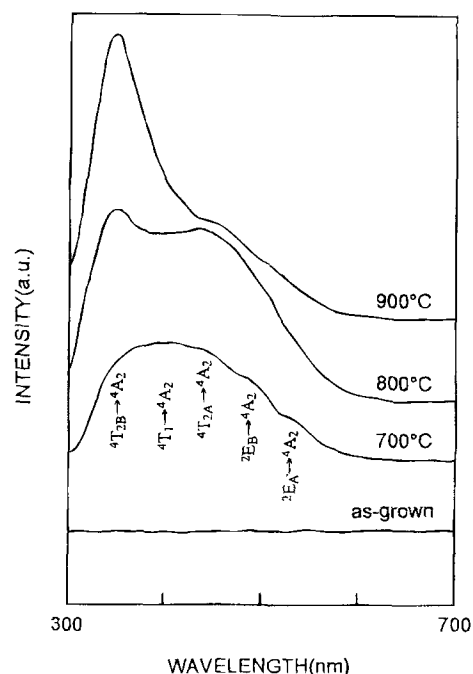


Fig. 9. Room temperature LVCL (500 V) spectra of ZnGa₂O₄ films (150 W, 4 mTorr, Ar/O₂ = 18/2, and no substrate heating) annealed at 700, 800, and 900°C for 3 h, respectively.

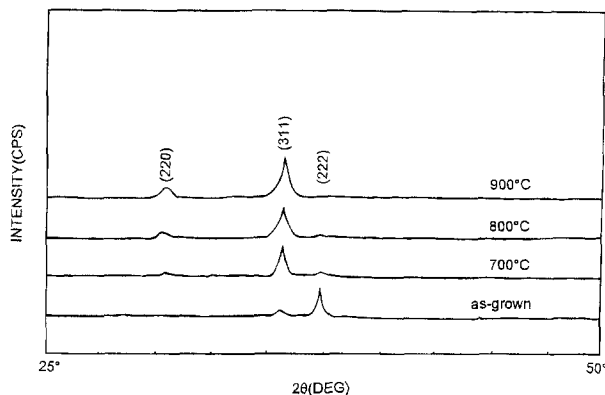


Fig. 10. XRD patterns of ZnGa_2O_4 films (150 W, 4 mTorr, $\text{Ar}/\text{O}_2 = 18/2$, and no substrate heating) annealed at 700, 800, and 900°C for 3 h, respectively.

Ga^{3+} ion. However, if this same ion is located on a Zn^{2+} site in spinel structure, it is surrounded by the six oxygens in the distorted octahedral configuration. The geometrical arrangements of the five 3d orbitals now become significant, since the interactions with the orbitals of the six oxygen ligands will produce shifts in the energy levels of the individual orbitals. The energy levels split, so that the five 3d levels no longer had the same energy. The splitting arrangement is controlled by the symmetry. Because the Ga^{3+} ions are not just on the octahedral sites may be on the tetrahedral sites after annealing treatment. We propose the energy level diagram of distorted octahedral structure. The transitions between ${}^4\text{T}_1$, ${}^4\text{T}_{2A}$, ${}^4\text{T}_{2B}$, ${}^2\text{E}_B$, and ${}^2\text{E}_A$ are just nonradiative reactions, for example energy transferred into other electrons for jumping higher level or vibration, etc. The only radiative process is falling to ${}^4\text{A}_2$ level for photon emission. So we could find four or five peaks in LVCL spectra. But different annealing treatments may lead to differ-

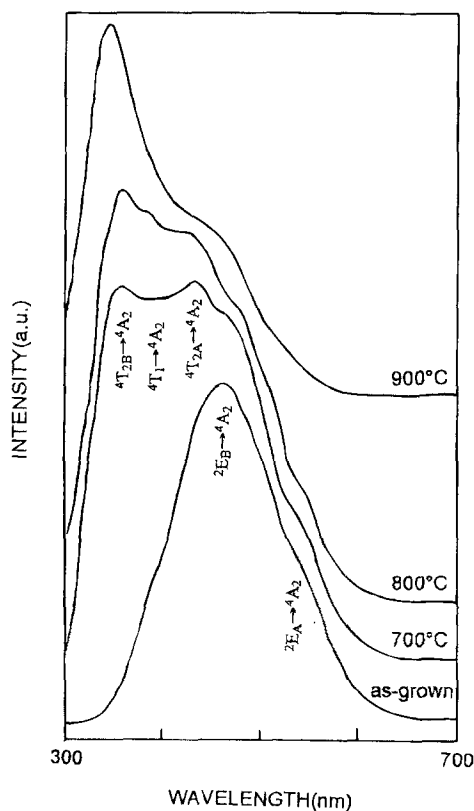


Fig. 11. Room temperature LVCL (500 V) spectra of ZnGa_2O_4 films (150 W, 4 mTorr, $\text{Ar}/\text{O}_2 = 18/2$, and 600°C substrate heating) annealed at 700, 800, and 900°C for 3 h, respectively.

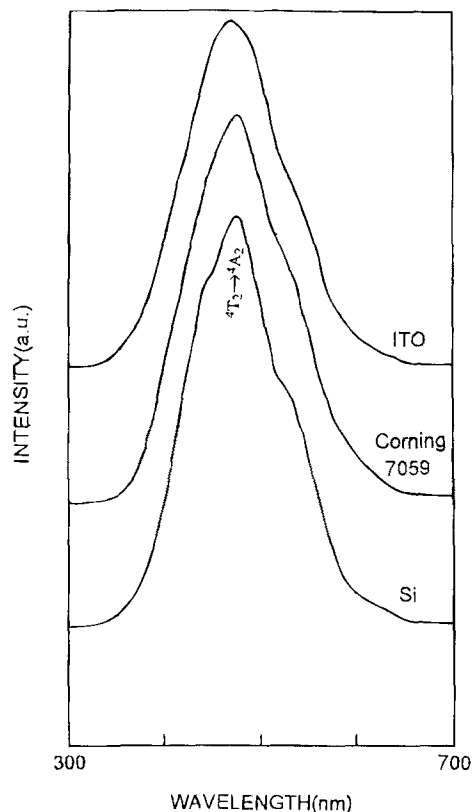


Fig. 12. Room temperature LVCL (500 V) spectra of ZnGa_2O_4 films (150 W, 4 mTorr, $\text{Ar}/\text{O}_2 = 18/2$, and 500°C substrate heating) deposited on different substrates (Si, Corning 7059, and ITO).

ent dominant levels. In Fig. 11, after the annealing treatment at 900°C for 3 h the dominant transition peak shifts to 360 nm. Moreover, the ${}^2\text{E}$ state acted as an energy reservoir for emission.¹⁹ We could take ${}^2\text{E}$ state as sensitizer level. When the broadened spectra of the sensitizer and activator overlap, resonant transfer of energy between them takes place. The mechanism of energy transfer between the sensitizer and the activator has been the subject of many experimental and theoretical investigations.²⁰⁻²² Usually, the efficiency of a phosphor can be improved by sensitizer levels.

We find a tendency that ZnGa_2O_4 phosphors with the higher x-ray intensity of (311) peak will lead to higher CL luminescent intensity. The (311) peak is the characteristic main peak of standard ZnGa_2O_4 powder diffraction pattern. It may be concluded that the films with the standard ZnGa_2O_4 x-ray diffraction pattern lead to better cathodoluminescence characteristics.

Usually, the orientation of deposited films is dependent on the crystalline orientation of substrate. Figure 12 shows the LVCL spectra of ZnGa_2O_4 phosphors on different substrates (Si, Corning 7059, and ITO). We can see the similar results of the x-ray pattern although the substrates are different. Different substrates will not affect the intensity of low voltage cathodoluminescence. This advantage will promote the development of ZnGa_2O_4 phosphor for future application.

Conclusion

Several parameters influencing the preferred orientation of sputtered ZnGa_2O_4 films are investigated in detail. The luminescent characteristics of phosphor films may be improved by the substrate heating and annealing treatment. High power or high growth temperature will enhance the crystallinity of ZnGa_2O_4 films. Moreover, they will lead to a large Ga/Zn relative atomic ratio. In addition, high power results in a large deposition rate. The oxygen environment is necessary for achieving the phosphor films with good crystallinity.

Better luminescent properties were observed on the films with the standard powder ZnGa_2O_4 x-ray diffraction pattern. Also, the substrate temperature above 500°C leads to the films with the standard powder ZnGa_2O_4 x-ray diffraction pattern. The effect of the strength of the ligand field on the resulting energy levels, labeled by their spectroscopic terms $^4\text{A}_2$, $^4\text{T}_1$, $^4\text{T}_2$, and ^2E . The main transition between the excited state ($^4\text{T}_2$) and luminescent center ($^4\text{A}_2$) is 2.64 eV of blue light emission (470 nm).

Uniform ZnGa_2O_4 phosphor films deposited by magnetron sputtering at proper pressure and power are obtained. Good luminescent characteristics of low voltage cathodoluminescence phosphor films are observed in this research.

Manuscript submitted Sept. 13, 1993; revised manuscript received Jan. 18, 1994.

Chung-Hua Polytechnic Institute assisted in meeting the publication costs of this article.

REFERENCES

1. S. Itoh, T. Kimizuka, and T. Tonegawa, *This Journal*, **136**, 1819 (1989).
2. S. Itoh, H. Toki, Y. Sato, K. Morimoto, and T. Kishino, *ibid.*, **138**, 1509 (1991).
3. K. Akagi, H. Kukimoto, and T. Nakayama, *J. Lumin.*, **17**, 237 (1978).
4. S. Oda, K. Akagi, H. Kukimoto, and T. Nakayama, *ibid.*, **16**, 323 (1978).
5. H. Kukimoto, S. Oda, and T. Nakayama, *ibid.*, **19**, 365 (1979).
6. S. Faria, *This Journal*, **135**, 2627 (1988).
7. S. Itoh, T. Tonegawa, and K. Morimoto, *ibid.*, **134**, 2628 (1987).
8. B. Chapman, *Glow Discharge Processes*, p. 177, John Wiley & Sons, Inc., New York (1980).
9. J. L. Vossen and W. Kern, *Thin Film Processes*, p. 77, Academic Press, Inc., New York (1978).
10. *Handbook of Thin Film Technology*, L. I. Maissel and R. Glang, Editors, McGraw-Hill, Inc., New York (1970).
11. R. J. Hill, *Physical Vapor Deposition*, Appendix C, Airco, Inc., California (1976).
12. H. M. Kahan and R. M. Macfarlane, *J. Chem. Phys.*, **54**, 5197 (1971).
13. J. A. Dauffy, *Bonding Energy Levels and Bands in Inorganic Solids*, p. 26, John Wiley & Sons, Inc., New York (1990).
14. K. Nassau, *The Physics and Chemistry of Color*, p. 83, John Wiley & Sons, Inc., New York (1983).
15. D. L. Wood, G. F. Imbusch, R. M. Macfarlane, P. Kisiuk, and D. M. Larkin, *J. Chem. Phys.*, **48**, 5255 (1968).
16. C. J. Donnelly, S. M. Healy, T. J. Glynn, G. F. Imbusch, and G. P. Morgan, *J. Lumin.*, **42**, 119 (1988).
17. W. Nie, F. M. Michel-Calendini, C. Linares, G. Boulou, and C. Daul, *ibid.*, **46**, 177 (1990).
18. R. Mlcak and A. H. Kitai, *ibid.*, **46**, 391 (1990).
19. H. M. Kahan and R. M. Macfarlane, *J. Chem. Phys.*, **54**, 5197 (1971).
20. R. Mlcak and A. H. Kitai, *J. Lumin.*, **46**, 391 (1990).
21. F. A. Kröger, *Physica*, **15**, 801 (1949).
22. D. L. Dexter, *J. Chem. Phys.*, **21**, 836 (1953).

Numerical Calculations of the Electrical Effects Induced by Structural Imperfections on MOS Capacitors

M. C. Valente Lopes and C. M. Hasenack

LSI/PEE/EPUSP, CEP 05508-900, São Paulo, SP, Brazil

V. Baranauskas

DSIF/FEE/UNICAMP, c.p. 6101, CEP 13081, Campinas, SP, Brazil

ABSTRACT

As the thickness of gate quality SiO_2 is reduced, minor structural interface imperfections begin to play an important role in device performance and yield. To isolate the effects of a variety of such interface imperfections on electric field distribution within the SiO_2 layer of biased metal oxide semiconductor capacitors, numerical calculations were carried out. The results indicate that strong electric field distortions may be expected for almost any interfacial defect configuration, being highest for metal precipitates. Technological consequences of the findings are also discussed.

The study of the high-field breakdown of thin SiO_2 layers has become an important issue because, due to the down-scaling of the geometry of microelectronics devices, without the appropriate scaling of the supply voltages, the devices are submitted to higher electric fields which enhance the probability of charge injection into the gate oxide thus leading to the possibility of accelerated degradation of the SiO_2 layer and of the Si- SiO_2 interface.

On actual metal/oxide/semiconductor (MOS) devices the gate oxide thickness may vary, say, between 5 and 20 nm. For such kinds of devices, the degree of uniformity and homogeneity of the SiO_2 bulk properties as well as those of the interfaces MOS is important for the adequate performance of the device. SiO_2 bulk defects play a fundamental role on the final performance and yield of modern devices. They have been extensively investigated,¹⁻⁷ and it was demonstrated that they can be effectively suppressed if appropriate precautions are taken. In that case the interface or surface properties (roughness and surface defects)

become of an increasing importance as far as high-field breakdown is concerned,^{8,9} demanding, therefore, increased attention.

With regard to this latter point, it is of interest to note the difficulty in assessing the electrical effect of the presence of a single defect on device characteristics. For example, microscopic defects such as microasperities are quite easily detected by atomic force microscopy (AFM), and there exists even a correlation between the presence of a collectivity of such asperities (numerically quantified as roughness) and device characteristics.¹⁰ But there is still a lack of a well-established correlation between a single, nanometer-sized, defective spot and the effect(s) it causes on device performance. Numerical calculations, however, constitute an exciting tool for approaching that problem because they allow one to isolate and to investigate the effect of a single defect on the performance of simple devices. Because numerical calculations usually allow one to carry out a two-dimensional analysis, the geometrical effect of the single defect can be investigated.